Available online at www.sciencedirect.com
SCIENCE DIRECT
Catalysis Today 114 (2006) 281–286
CATALYSIS TODAY
www.elsevier.com/locate/cattod

WGS and reforming properties of NbMCM-41 materials

Izabela Sobczak [a], Joanna Goscianska [a], Maria Ziolek [a,*], Jacek Grams [b], Christelle Verrier [c], Philippe Bazin [c], Olivier Marie [c], Marco Daturi [c,*]

[a] *Adam Mickiewicz University, Faculty of Chemistry, Grunwaldzka 6, 60-780 Poznań, Poland*
[b] *Institute of General & Ecological Chemistry, Technical University of Łódź, Żeromskiego 116, 90-924 Łódź, Poland*
[c] *Laboratoire Catalyse et Spectrochimie, UMR 6506 CNRS, ENSICaen and Université de Caen Basse-Normandie, 6, Boulevard Maréchal Juin, 14050 CAEN Cedex, France*

Available online 20 February 2006

Abstract

NbSiMCM-41 and Pt/NbSiMCM-41 samples were characterised from the structural and morphological point of view. FT-IR studies allowed to evidence Water Gas Shift and reforming phenomena, taking place after CO introduction in the presence of an hydrated surface. The reactivity of the system and the role of the support towards hydrogen production were discussed on the base of infrared and TOF-SIMS results.

Keywords: NbSiMCM-41; Pt/NbSiMCM-41; TOF-SIMS; WGS and reforming properties

1. Introduction

The actual environmental problems have pushed the researchers to develop new transport systems. Among them, fuel cells fed by hydrogen seem to be a valuable alternative for energy production. H_2 extraction from hydrocarbons (especially light alkanes) via Water Gas Shift or reforming has therefore become a main goal in nowadays catalysis. The most active materials for these kinds of reactions seem to be Pt-supported catalysts. MCM-41 mesoporous molecular sieves, due to their uniform molecular structure and high surface area that could provide a better dispersion of the active sites, are attractive new supports for Pt. On the other hand, the presence of Nb in NbSiMCM-41 matrix enhances the oxidative properties of the catalyst [1]. Moreover, Nb is well known for its reforming properties. It was found that Pt/Nb_2O_5 shows high activity and selectivity for benzene in the dehydrogenation of cyclohexane [2,3], and Nb_2O_5/Al_2O_3 is an active catalyst for the isomerisation of 1-butene [4]. In the present paper, we show interesting performances of mesoporous molecular sieves containing niobium and platinum.

2. Experimental

2.1. Samples preparation—synthesis and modification

SiNb-containing mesoporous molecular sieve of MCM-41 type was synthesised according to the procedure described in [5] and modified in the preparation of NbSiMCM-41 according to [6]. Si/Nb atom ratio was 128 as assumed.

The Pt/NbSiMCM-41 catalyst was prepared by impregnation of NbSiMCM-41 support with an aqueous solution of chloroplatinic acid ($H_2PtCl_6{\cdot}6H_2O$ hydrogen hexachloroplatinate(IV) hydrate—Aldrich) with a platinum loading of 1 wt.%. The obtained material was dried at 373 K for 5 h, calcined at 773 K for 3 h in air and reduced in H_2 (5 vol.% H_2 in N_2) at 773 K for 3 h.

2.2. Samples characterisation

The surface area and pore volume of the MCM-41 materials were measured by nitrogen adsorption at 77 K using the conventional technique on a Micromeritics 2010 apparatus. Prior to the adsorption measurements, the samples were degassed in vacuum at 573 K for 2 h. Surface area was calculated by the BET method. The pore size and the mesopore volume were determined from the adsorption isotherms using a corrected algorithm (KJS–BJH) based on the Barret–Joyner–Halenda (BJH) procedure [7].

* Corresponding authors. Tel.: +48 61 829 1243; fax: +48 61 865 8008.
E-mail addresses: ziolek@amu.edu.pl (M. Ziolek), Marco.Daturi@ensicaen.fr (M. Daturi).

0920-5861/$ – see front matter
doi:10.1016/j.cattod.2006.01.017

The XRD patterns were obtained on a TUR-62 diffractometer using Cu Kα radiation (λ = 0.154 nm).

The time-of-flight secondary ion mass spectrometry (TOF-SIMS) investigations were performed using an ION-TOF instrument (TOF-SIMS IV) equipped with a 25 kV pulsed $^{69}Ga^+$ primary ion gun in the static mode. To obtain the plain surface of catalysts, powder samples were tableted before the measurements. Tablets were attached to the sample holder using a double-sided tape. For each sample three spectra and images were collected (from different areas). The analysed area corresponds to a square of 500 μm × 500 μm. For charge compensation a pulsed electron flood-gun was used.

2.3. Sample FTIR characterisation

Material surface properties have been studied by in situ FT-IR spectroscopy of adsorbed probe molecules, using sample wafers of 5 mg cm^{-2} analysed in a classical quartz cell. Spectra were recorded at room temperature with a Nicolet Magna 550 FT-IR spectrometer (resolution 4 cm^{-1}) after quenching the samples to room temperature. Probe molecules (CO, CH_3OH) were introduced at room temperature on the activated samples (activation at 723 K under vacuum) and then evacuated. The spectra have been treated by the Nicolet OMNIC™ software.

IR studies in flow system were performed using a commercial Spectratech DRIFT reactor-cell (placed in a Nicolet Magna 750 FTIR spectrometer) connected to a flow set-up. It allows simultaneous observation of adsorbed surface species and gas products, both in steady state and transient conditions. Gas products are in fact analysed by FTIR via a gas micro-cell (multireflection cell with an inner volume of 88 μl) and by mass spectrometry (Balzers TCP121). Further details about these coupled techniques can be found in reference [8].

3. Results

3.1. Characterisation of the catalysts

The mesoporous molecular sieves of MCM-41 type studied in this work base on silicate framework, in which silicon is partially isomorphous substituted by niobium (Si/Nb = 128). NbSiMCM-41 was applied as a support for platinum to obtain a Pt/NbSiMCM-41 material. The samples were analysed from the point of view of structural, textural, morphological and surface properties.

The data calculated from N_2 adsorption isotherms are shown in Table 1. Both materials – NbSiMCM-41 and Pt/NbSiMCM-41 – possess high surface areas and pore volumes. These parameters as well as pore diameters only slightly decrease after Pt impregnation of NbSiMCM-41. The prepared MCM-41 samples exhibit the N_2 adsorption/desorption isotherms of type IV (IUPAC) (not shown here) typical of mesoporous materials.

Table 1
Textural data of the catalysts used

Catalyst	Surface area BET ($m^2\ g^{-1}$)	Mesopore volume BJH-KJS ($cm^3\ g^{-1}$)	Pore diameter BJH-KJS (nm)
NbSiMCM-41	961	0.83	3.6
Pt/NbSiMCM-41	910	0.74	3.3

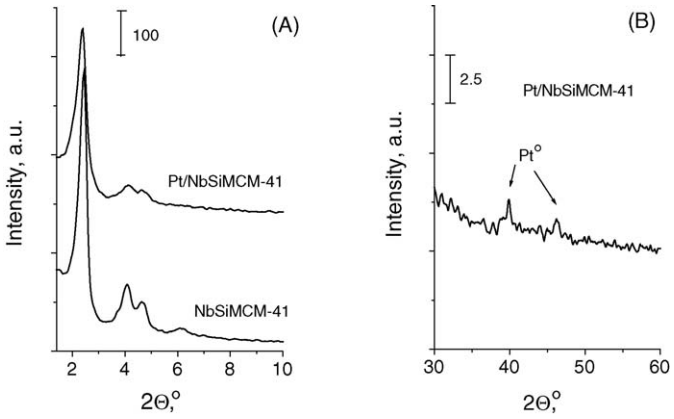

Fig. 1. (A and B) XRD patterns of MCM-41 materials.

The powder X-ray diffraction pattern (Fig. 1A) of the parent NbSiMCM-41 material is consistent with the X-ray powder diffraction patterns of MCM-41 reported in the literature [5]. It is characterised by a narrow single peak [1 0 0] centred at $2\theta \approx 2^\circ$ and by up to three well resolved reflections in the region of $2\theta = 3–8^\circ$ typical of hexagonal ordered mesoporous tubes. The XRD pattern of Pt/NbSiMCM-41 is slightly affected by the modification with Pt-acid (Fig. 1A). The intensity of XRD reflections between $2\theta = 3–8^\circ$ decreases indicating the small disordering in the long-range of the hexagonal structure.

It is worthy of notice, that Pt-metal clusters can be estimated from XRD patterns. For Pt/NbSiMCM-41 the peaks at $2\theta = 39.6^\circ$ and 46.2° characteristic of metallic platinum are visible (Fig. 1B). The peaks at 39.7° and 46.2° origins from (1 1 1) and (2 0 0) planes, respectively [9].

Fig. 2 presents negative (A) and positive (B) secondary ion mass spectrum of NbSiMCM-41 material. The signals visible on the mass spectrum at the *m/z* range from 28 to 77 were ascribed to the presence of Si^-, SiH^-, SiO_x^- and SiO_xH^- ($x = 1–3$) ions, which originate from the catalyst surface (Fig. 2A). The Nb containing ions (Nb^+, NbO^+, NbO_2^+) were observed on the positive secondary ion mass spectrum of NbSiMCM-41 (Fig. 2B). The observation of niobium isolated species as well as Nb-O groups has an important impact in the further consideration of WGS and reforming process on NbSiMCM-41 material (free from Pt).

The negative secondary ion mass spectrum of Pt/NbSiMCM-41 catalyst is shown in Fig. 2C. In this case the following Pt containing ions were distinguished: Pt^-, PtO^-, PtO_2^-, $PtCl^-$ and $PtClO^-$. This fact indicates that a certain number of Pt atoms placed on the catalyst surface can interact with Cl and owing to that Pt-Cl and Pt-O-Cl clusters are observed on the mass spectrum [10].

The comparison of the emission intensities for the Si and Nb containing ions present in both samples (NbSiMCM-41, Pt/NbSiMCM-41), allowed the calculation of the ion intensity ratios; the results are summarized in Table 2. For comparison the data for calcined Pt/NbSiMCM-41 are also included into the

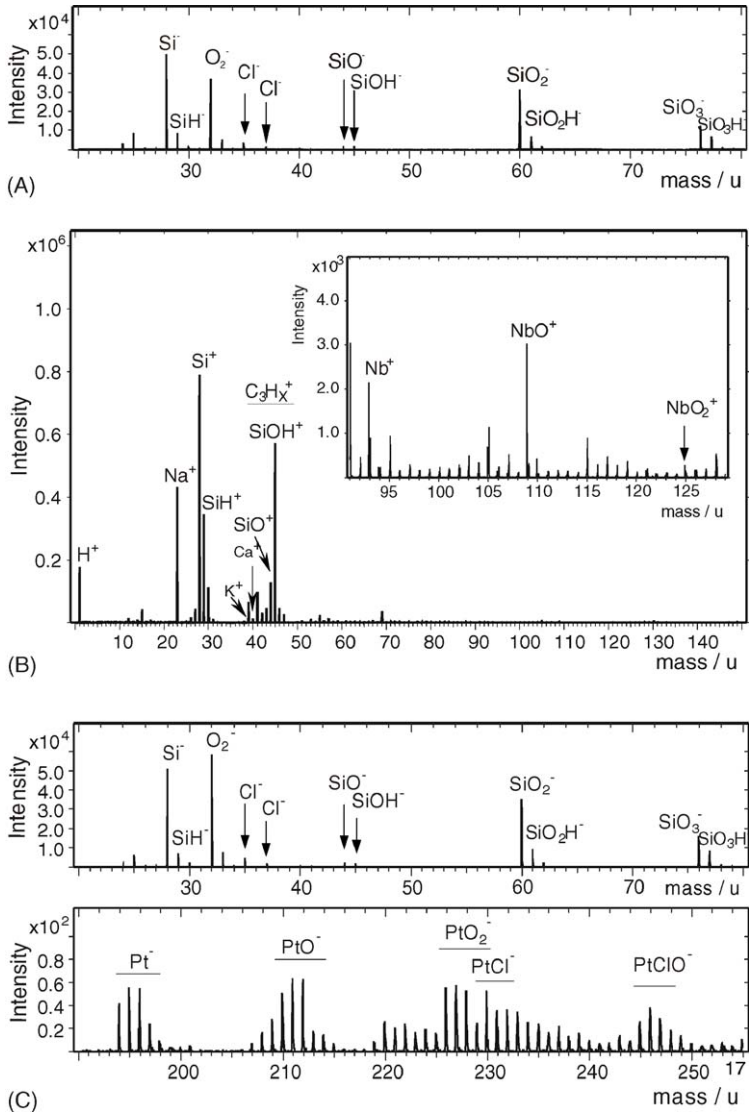

Fig. 2. Fragments of negative (A) and positive (B) TOF-SIMS spectrum of NbSiMCM-41 catalyst; the fragment of negative TOF-SIMS spectrum of Pt/NbSiMCM-41 catalyst (C).

table. The values of $SiOH^-/SiO^-$, SiO_2H^-/SiO_2^-, $SiOH_3^-/SiO_3^-$, NbO_2^+/Nb^+ and NbO_2^+/NbO^+ intensity ratios are similar in all cases and do not noticeably change after addition of Pt and further catalyst reduction in comparison to the calcined support. It indicates that an applied treatment (reduction in H_2 at 773 K for 3 h) of the investigated catalyst and the presence of Pt do not influence significantly the properties of the support surface (the number of O and H atoms in the surroundings of Si or Nb remains almost on the same level). The only exception is NbO^+/Nb^+ ratio which decreases after Pt loading followed by calcination. It suggests that a part of oxygen from NbO species is active in the transformation of surface species.

Table 2
The TOF-SIMS intensity ratios of selected ions

Intensity ratios	NbSiMCM-41 (after calcination)	Pt/NbSiMCM-41 (after calcination)	Pt/NbSiMCM-41 (after reduction)
$SiOH^-/SiO^-$	1.17	1.12	1.23
SiO_2H^-/SiO_2^-	0.21	0.21	0.22
SiO_3H^-/SiO_3^-	0.54	0.55	0.55
NbO^+/Nb^+	1.28	1.12	1.08
NbO_2^+/Nb^+	0.14	0.13	0.13
NbO_2^+/NbO^+	0.11	0.12	0.12
Cl^-/H^-	6.3×10^{-3}	1.1×10^{-2}	1.0×10^{-2}

The high sensitivity obtained during TOF-SIMS measurements allowed to observe the presence of surface impurities. In the case of NbSiMCM-41 matrix and Pt/NbSiMCM-41 catalyst a certain amount of Na, K, Ca and Cl were noticed, certainly belonging to residuals of the precursors. Moreover, the comparison of Cl content showed that the quantity of Cl (Table 2) on the Pt-containing catalyst surface was noticeable bigger (≈twice) than for the support. That increase of Cl amount may be connected with the process of Pt introduction (from the H_2PtCl_6) on the surface during the catalyst preparation.

The surface image of the Pt/NbSiMCM-41 catalyst is given in Fig. 3. It indicates a good distribution of Nb on the surface and good dispersion of Pt. Although platinum signal is weak because of a high ionisation energy for this metal, it seems to be

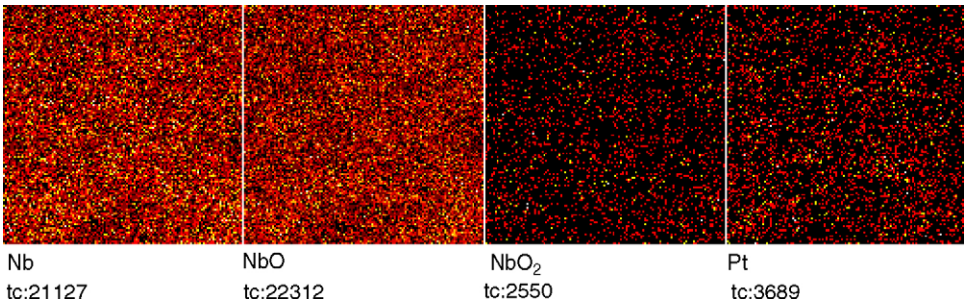

Fig. 3. TOF-SIMS high resolution image of Pt/NbSiMCM-41 catalyst. Bright colour indicates investigated ions.

uniformly distributed on the support surface (bright colour on the images indicates the existence of the pointed ion). Recently, the high dispersion of Pt on the Pt/NbSiMCM-41 catalyst after reduction in H_2 was confirmed by TEM measurements [11]. The average size of Pt particles was estimated at 5–10 nm. However, the fraction of smaller particles with sizes up to 2 nm dominated (about 60%) [12].

3.2. WGS and reforming properties

A Pt/NbSiMCM-41 catalyst was submitted to in situ IR analysis with the aim to test platinum dispersion by CO adsorption [13]. Prior to the experiment, the sample was activated by heating at 723 K under oxygen (to remove eventual template traces), then vacuum. Successively, a reducing treatment under hydrogen at 423 K was performed to reduce the supported metal. In these conditions platinum is fully reduced to Pt^0 and platinum metal particles are prevented from migration and agglomeration at that temperature. In fact, a little higher temperature (473 K) is sufficient for totally reducing platinum even on redox ceria support, as discussed in [13]. As soon as the first CO dose (2.22×10^{-8} mol) was introduced into the cell, a band appeared at 2060 cm^{-1} (see Fig. 4), assigned to CO linearly coordinated on Pt small particles [14]. CO_2 and water were also formed, as shown by the bands at 2349 and 1636 cm^{-1}. Their production

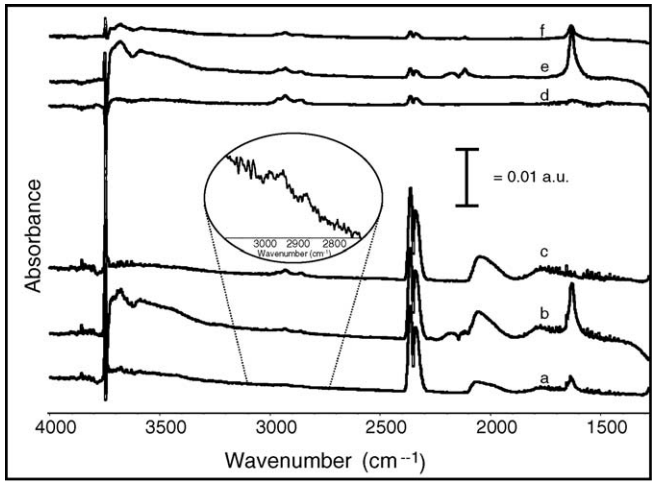

Fig. 4. IR difference spectra of Pt/NbSiMCM-41 sample after CO small dose introduction (a), CO saturation (b) and evacuation at rt (c), as well as NbSiMCM-41 sample after CO small dose introduction (d), CO saturation (e) and evacuation at rt (f).

was firstly attributed to CO partial oxidation on Pt unreduced sites and to OH perturbation, respectively, as it was also confirmed by the changes in the hydroxyl bands in the 3800–3300 cm^{-1} region. Better scrutinizing the spectrum, vibrations in the ν(CH) stretching region were revealed (see zoom), which grew up by adding CO doses (Fig. 4, spectrum b). Band position at 2961, 2928, 2860 cm^{-1} (and at 1465, 1447 cm^{-1} for bending modes) suggests that such adsorbed species are methoxy groups, as it was further confirmed by methanol adsorption on the activated sample.

Also the NbSiMCM-41 sample presents the same behaviour, accompanied by even more intense bands (Fig. 4, spectra d–f). To ascertain the extent of the production of such species and eventually the presence of other compounds not visible by IR, we tested the samples in a system currently used for *operando* studies, under a CO flow, using Ar as a gas vector. Before that, activation was performed with $Ar + O_2$ (10 vol.%) at 523 K in order to remove the traces of the template. Next, $Ar + H_2$ (10 vol.%) was passed through the catalyst at 523 K to reproduce the in situ conditions. In such a case not true *operando* conditions were applied, but the system currently used for real *operando* studies was employed for on-line analyses by IR spectroscopy and mass spectrometry. After the activation, the catalyst was left under Ar at 523 K to remove the rest of hydrogen and next it was exposed to the reaction stream at increasing temperatures. Mass spectra showed hydrogen production concomitantly with $CO \rightarrow CO_2$ oxidation (Fig. 5) and hydroxyls consumption was seen from IR spectra (not shown here) when the temperature reached 523 K. On the contrary, by IR analysis we could not put

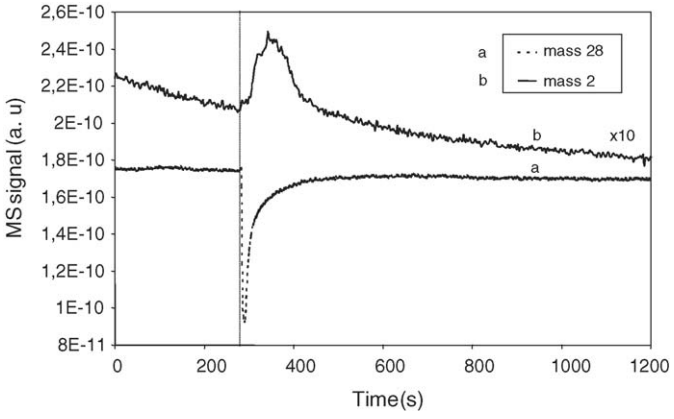

Fig. 5. MS profile for masses 28 (CO) and 2 (H_2) after CO introduction in an Ar stream on NbSiMCM-41 sample at 523 K.

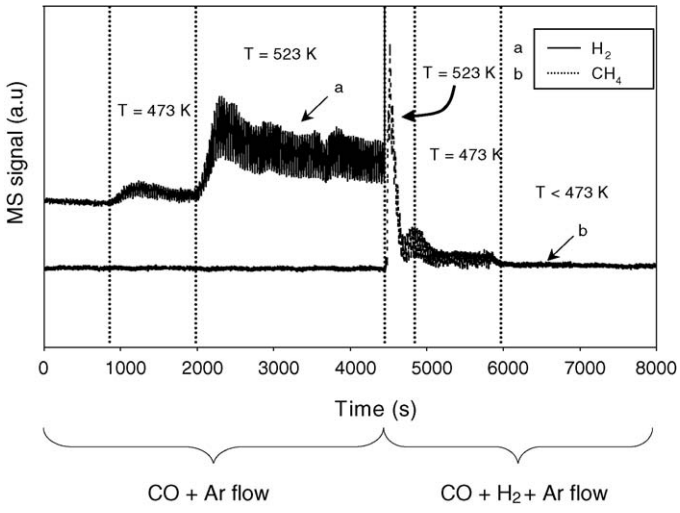

Fig. 6. MS profile for hydrogen and methane after CO or CO + H_2 introduction in an Ar stream on Pt/NbSiMCM-41 sample at different temperatures.

in evidence methanol formation, perhaps due to the too high temperature, leading to species decomposition. The same experiment was repeated on the Pt/NbSiMCM-41 sample: again hydrogen was produced under CO flow, but already at 473 K (Fig. 6). At 523 K H_2 output was observed to be greater; it was maintained almost constant by water introduction in the stream. Again, no methanol formation could be detected in these conditions. Nevertheless, a reaction flow containing CO + H_2 + Ar gave rise to methane formation in the 523–473 K range of temperatures, whereas for $T < 473$ K that species disappeared (Fig. 6).

4. Discussion

From the results reported above, it appears that WGS and reforming phenomena have happened on the analysed sample. We could suggest that the following reactions have taken place:

$$CO + 2M\text{-}OH \rightarrow CO_2 + H_2O + M \quad (1)$$

where M = matrix

$$CO + H_2O \rightarrow CO_2 + H_2 \quad (2)$$

$$CO + 2H_2 \rightarrow CH_3OH \quad (3)$$

Reaction (1) was clearly observed in the in situ IR spectra via hydroxyl consumption and CO_2–water formation (Fig. 4). Reaction (2) was evidenced by MS analysis in the *operando* system. We can therefore confirm that WGS phenomena can occur on Nb-substituted mesoporous MCM-41 materials.

Pt loaded oxides are well known to produce these kinds of reactions [15]. In the present case, NbSiMCM-41 matrix for Pt seems to play a similar role as ceria in the WGS and reforming process [16–20]. Generally two mechanisms for WGS process on Pt/CeO_2 are considered: (i) a redox process in which Pt is an active centre for CO chemisorption, ceria is reduced producing CO_2 and next it is reoxidised in the interaction with H_2O which is accompanied by hydrogen formation; (ii) the reaction of hydroxyl groups from reduced ceria with CO produces formate species, which decomposes towards hydrogen. In the case of our study water is formed upon the interaction of CO with hydroxyl groups from the NbSiMCM-41 matrix. When Pt/NbSiMCM-41 catalyst is used, CO is chemisorbed on Pt species (the Pt-CO complex was registered in the IR spectra—Fig. 4) and in this form it interacts with NbSiMCM-41 matrix leading to the abstraction of oxygen from Nb-O groups present on the surface. Nb in NbMCM-41 is coordinated to four oxygen atoms in the skeleton and one on the surface [1]. The latter is mobile and easily interacts with CO chemisorbed on platinum species. This process leads to the formation of CO_2 and four coordinated $Nb^{\delta+}$ species. Water is chemisorbed on the latter species and finally hydrogen is formed. Methoxy species can therefore result from the reaction between CO and H_2:

$$M\text{-}Pt + CO \rightleftarrows M\text{-}Pt\text{-}CO \quad \text{where M} = \text{matrix}$$

$$M\text{-}Pt\text{-}CO + M\text{-}Nb\text{-}O \rightleftarrows M\text{-}Pt + M\text{-}Nb + CO_2$$

$$M\text{-}Nb + H_2O \rightleftarrows M\text{-}Nb\text{-}OH_2$$

$$M\text{-}NbOH_2 \rightleftarrows M\text{-}Nb\text{-}O + H_2$$

$$CO + 2H_2 \rightarrow CH_3OH$$

For Pt-free sample, NbSiMCM-41, niobium isolated species identified earlier [21] as $Nb^{\delta+}$ are supposed to give rise to the formation of Nb-CO complex, which cannot be easily observed in IR spectra [22]. Therefore, one can suppose that Nb-O species, which was characterized in this work (Fig. 2B) and found earlier [1,21] as the source of active oxygen, interacts with CO forming CO_2, whereas $Nb^{\delta+}$ species interacts with H_2O (and hydrogen is so formed):

$$M\text{-}Nb\text{-}O + CO \rightleftarrows M\text{-}Nb\text{-}O\text{-}CO$$

$$M\text{-}Nb\text{-}O\text{-}CO \rightleftarrows M\text{-}Nb + CO_2$$

$$M\text{-}Nb + H_2O \rightleftarrows M\text{-}Nb\text{-}OH_2$$

$$M\text{-}Nb\text{-}OH_2 \rightleftarrows M\text{-}Nb\text{-}O + H_2$$

It is worthy of notice that $Nb^{\delta+}$ species already exist in the parent NbSiMCM-41 material [21]. Therefore, the production of hydrogen from the interaction of these species with H_2O is much faster then the route via interaction of Nb-O species with chemisorbed CO. That causes the formation of H_2 at the beginning of the reaction. Then hydrogen interacts with CO producing methoxy species. Being CO weaker held on the surface of NbSiMCM-41 than on Pt/NbSiMCM-41, its reactivity is enhanced, thus we can observe the formation of significant amount of methoxy species even after a CO small dose introduction (Fig. 4) on NbSiMCM-41.

Concerning reforming properties of the studied samples, even if in situ analysis could identify methoxy species on both samples, reaction (3) could not be demonstrated under flow. Probably this is due to the fact that in the steady state, under controlled atmosphere, CH_3O species are relatively stable,

whereas under stream (at rather high temperature compared to in situ experiments) they probably decompose. In any case their concentration is small on the surface of the catalysts, so that the amount of eventually produced methanol is probably under the detection edge. Nevertheless the reforming capacities of Pt/NbSiMCM-41 material have been evidenced by methane formation when a $CO + H_2$ flow is introduced in the cell. In these reducing conditions, the reaction should progress till the alkane formation.

5. Conclusions

- Water Gas Shift and reforming phenomena were distinctly observed on NbSiMCM-41 materials.
- Being the concentration of produced hydrogen or hydrocarbons relatively low, the direct application of such compounds to fuel cells is perhaps not reliable.
- Nevertheless, from the fundamental point of view, it has been extremely interesting to get a deeper view inside the reaction mechanism. In particular, we have advanced the hypothesis that the Nb redox properties play a major role inside WGS phenomena as it is the case for ceria based compounds.
- Some reaction steps leading to hydrogen formation on such catalysts were proposed.

Acknowledgements

State Committee for Scientific research (KBN—grant no. 3T09A 100 26; 2004–2007) is acknowledged for a partial support of this work. Acknowledge is made to CBMM (Brasil) for supplying niobium(V) oxalate.

References

[1] M. Ziolek, I. Sobczak, A. Lewandowska, I. Nowak, P. Decyk, M. Renn, B. Jankowska, Catal. Today 70 (2001) 169.
[2] D.A.G. Aranda, A.L.D. Ramos, F.B. Passos, M. Schmal, Catal. Today 28 (1996) 119.
[3] F.B. Passos, D.A. Aranda, R.R. Soares, M. Schmal, Catal. Today 43 (1998) 3.
[4] S. Hasegawa, H. Aritani, M. Kudo, Catal. Today 16 (1993) 371.
[5] C.T. Kresge, M.E. Leonowicz, W.J. Roth, J.C. Vartuli, J.S. Beck, Nature 359 (1992) 710.
[6] M. Ziolek, I. Nowak, Zeolites 18 (1997) 356.
[7] M. Kruk, M. Jaroniec, A. Sayari, Langmuir 13 (1997) 6267.
[8] T. Lesage, C. Verrier, P. Bazin, J. Saussey, M. Daturi, Phys. Chem. Chem. Phys. 5 (2003) 4435.
[9] S.-C. Shen, S. Kawi, Appl. Catal. B-Environ. 45 (2003) 63.
[10] Y. Zhou, M.C. Wood, N. Winograd, J. Catal. 146 (1994) 82.
[11] I. Sobczak, M. Ziolek, M. Nowacka, Microporous Mesoporous Mater. 78 (2005) 103.
[12] I. Sobczak, M. Ziolek, J. Goscianska, F. Romero Sarria, M. Daturi, J.M. Jablonski, Stud. Surf. Sci. Catal. 158 (2005) 1319.
[13] V. Perrichon, L. Retailleau, P. Bazin, M. Daturi, J.C. Lavalley, Appl. Catal. A: Gen. 260 (2004) 1.
[14] P. Bazin, O. Saur, J.C. Lavalley, M. Daturi, G. Blanchard, Phys. Chem. Chem. Phys. 7 (2005) 187.
[15] A. Ghenciu, Curr. Opin. Solid State Mater. Sci. 6 (2002) 389.
[16] G. Jacobs, U.M. Graham, E. Chenu, P.M. Patterson, A. Dozier, B.H. Davis, J. Catal. 229 (2005) 499.
[17] L. Mendelovici, M. Steinberg, J. Catal. 93 (1985) 353.
[18] T. Shido, Y. Iwasawa, J. Catal. 141 (1993) 71.
[19] A. Goguet, F. Meunier, J.P. Breen, R. Burch, M.I. Petch, A. Faur Ghenciu, J. Catal. 226 (2004) 382.
[20] C. Wheeler, A. Jhalani, E.J. Klein, S. Tummala, L.D. Schmidt, J. Catal. 223 (2004) 191.
[21] M. Ziolek, I. Sobczak, I. Nowak, P. Decyk, A. Lewandowska, J. Kujawa, Microporous Mesoporous Mater. 35–36 (2000) 195.
[22] K.I. Hadjiivanov, G.N. Vayssilov, Adv. Catal. 33 (47) (2002) 307.